

Highly Emissive Self-Trapped Excitons in Fully Inorganic Zero-Dimensional Tin Halides

Bogdan M. Benin⁺, Dmitry N. Dirin⁺, Viktoriia Morad, Michael Wörle, Sergii Yakunin, Gabriele Rainò, Olga Nazarenko, Markus Fischer, Ivan Infante, and Maksym V. Kovalenko*

Abstract: The spatial localization of charge carriers to promote the formation of bound excitons and concomitantly enhance radiative recombination has long been a goal for luminescent semiconductors. Zero-dimensional materials structurally impose carrier localization and result in the formation of localized Frenkel excitons. Now the fully inorganic, perovskite-derived zero-dimensional Sn^{II} material Cs₄SnBr₆ is presented that exhibits room-temperature broadband photoluminescence centered at 540 nm with a quantum yield (QY) of 15 ± 5 %. A series of analogous compositions following the general formula Cs_{4-x}A_xSn(Br_{1-y}I)_y (A = Rb, K; x ≤ 1, y ≤ 1) can be prepared. The emission of these materials ranges from 500 nm to 620 nm with the possibility to compositionally tune the Stokes shift and the self-trapped exciton emission bands.

Interest in low-dimensional metal halide semiconductors,^[1] and ultimately their zero-dimensional (0D) counterparts,^[2] has been spurred by the increasing interest in 3D lead halide perovskites.^[3] In recent years, lead halide perovskites have risen to prominence in the field of optoelectronics with their use in full-color imaging,^[4] photodetection,^[5] X-ray imaging,^[6] hard-radiation detection,^[7] solar cells,^[8] and light-emitting diodes,^[9] owing to their defect-tolerant photophysics and charge transport.^[10]

As the dimensionality decreases, the metal halide octahedra become progressively less-connected and the optical and electrical properties shift away from those of a delocalized, 3D network towards 0D, molecular-like, isolated octahedra. In such structures, self-trapped excitons (STEs) form owing to the local deformation of the crystal lattice upon photo-excitation. This strong spatial localization, and the absence of electronic trapping processes that are inherent in electronically extended (higher-dimensionality) solids, favors radiative recombination. Previously, the spatial confinement of carriers in 3D perovskites has been attained through crystal size control at the nanoscale (that is, top-down and bottom-up synthesis of nanocrystals).^[11] In the case of 0D materials, such elaborate crystal size engineering is not required as the optical properties are instead governed by their structural dimensionality. Highly localized Frenkel-like excitons are formed instead of Wannier–Mott type excitons.

The library of 0D metal halides with octahedral building units includes both lead-based and lead-free compounds: Ti^{IV},^[12] Hf^{IV},^[13] Zr^{IV},^[14] Pd^{IV},^[15] Pb^{II},^[16] Sn^{IV},^[17] Te^{IV},^[18] Sb^{III},^[19] and Bi^{III}.^[20] However, only several of these examples exhibit photoluminescence (PL) at room temperature (RT), and this emission is seldom characterized by a high PL quantum yield (QY). The first examples with high QYs in excess of 50 % were demonstrated only recently: (C₄N₂H₁₄Br)₄SnBr₆ (QY = 95 % ± 5 %) and (C₄N₂H₁₄I)₄SnI₆ (QY = 75 % ± 4 %).^[21] Both structures are constructed from disconnected [SnX₆]⁴⁻ octahedra, separated by large organic cations with a distance of more than 1 nm between Sn²⁺ centers.

Given the high PL QY of these hybrid materials and their novel approach towards exciton localization, herein we chose to pursue fully inorganic analogues such as Cs₄SnBr₆. While several studies have reported on the structure and basic properties of Cs₄SnBr₆, none have observed PL at RT.^[22] Recently, calculations have shown that the Cs₄SnBr₆ phase should have a band gap of 3.37 eV.^[23] We prepared Cs_{4-x}A_xSn(Br_{1-y}I_y)_y (A = Rb, K) materials using a simple solid-state heat-and-beat approach, characterized them structurally, and found them to be luminescent at RT.

According to the CsBr–SnBr₂ pseudo-binary phase diagram (Figure 1a), Cs₄SnBr₆ melts incongruently and competes with the decomposition into the black CsSnBr₃ and CsBr. Therefore, phase-pure Cs₄SnBr₆ cannot be obtained by cooling from a melt of this composition. Instead, solid pellets of a mixture of CsBr (4.5 equiv.) and SnBr₂ (1 equiv.) were repeatedly heated to 350 °C for 60 h and reground in a glovebox between heating cycles. The highlighted green region in Figure 1a represents the experimental conditions that were found to yield the purest materials, that is, at temperatures

[*] B. M. Benin,^[+] Dr. D. N. Dirin,^[+] V. Morad, Dr. M. Wörle, Dr. S. Yakunin, Dr. G. Rainò, O. Nazarenko, M. Fischer, Prof. Dr. M. V. Kovalenko
Laboratory of Inorganic Chemistry, ETH Zürich
CH-8093 Zürich (Switzerland)
E-mail: mvkovalenko@ethz.ch

B. M. Benin,^[+] Dr. D. N. Dirin,^[+] V. Morad, Dr. S. Yakunin, Dr. G. Rainò, O. Nazarenko, Prof. Dr. M. V. Kovalenko
Laboratory for Thin Films and Photovoltaics
Empa—Swiss Federal Laboratories for Materials
CH-8600 Dübendorf (Switzerland)
Dr. I. Infante
Department of Theoretical Chemistry, Faculty of Science
Vrije Universiteit Amsterdam
de Boelelaan 1083, 1081 HV Amsterdam (The Netherlands)

[+] These authors contributed equally.

Supporting information and the ORCID identification number(s) for the author(s) of this article can be found under:
<https://doi.org/10.1002/anie.201806452>.

© 2018 The Authors. Published by Wiley-VCH Verlag GmbH & Co. KGaA. This is an open access article under the terms of the Creative Commons Attribution-NonCommercial License, which permits use, distribution and reproduction in any medium, provided the original work is properly cited and is not used for commercial purposes.

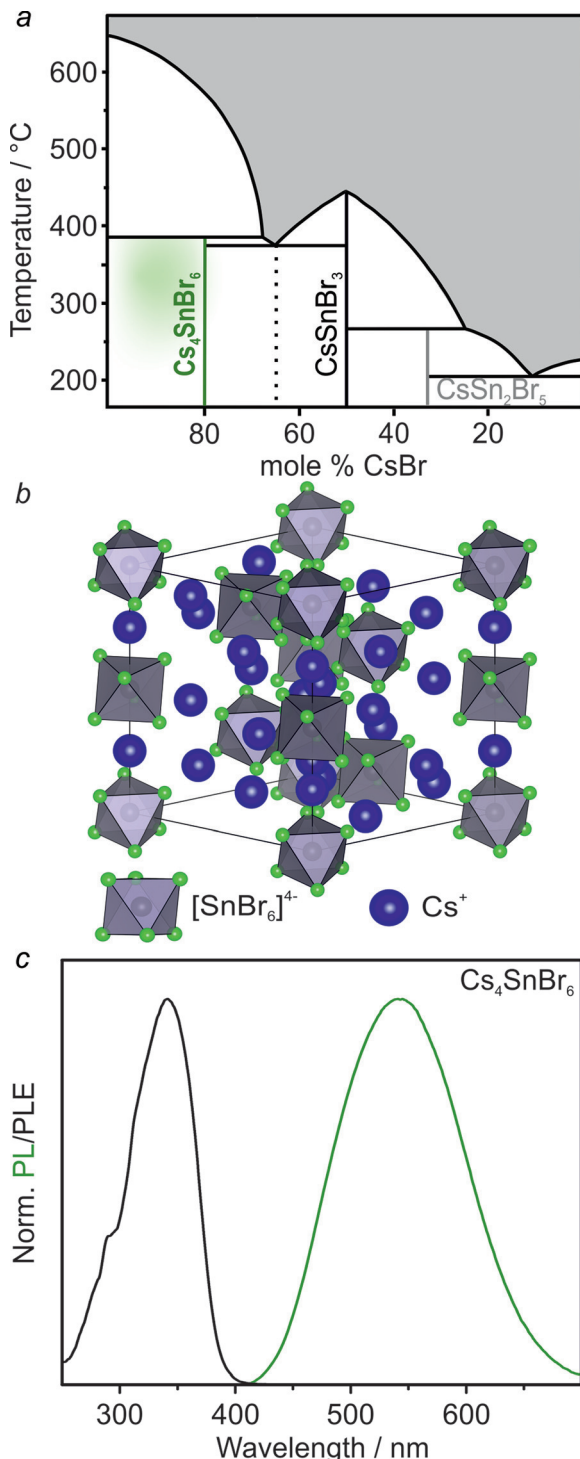


Figure 1. a) The pseudo-binary $\text{CsBr}-\text{SnBr}_2$ phase diagram.^[22a] The highlighted green region represents the experimental conditions found to yield the purest Cs_4SnBr_6 material. b) The crystal structure of Cs_4SnBr_6 viewed along the (111) axis with $[\text{SnBr}_6]^{4-}$ octahedra (gray with green bromine atoms) separated by Cs^+ cations (blue). c) PL and PLE spectra for Cs_4SnBr_6 at RT.

below the decomposition point of Cs_4SnBr_6 (Supporting Information, Figures S1, S2; Tables S1, S2). Single crystals of Cs_4SnBr_6 were obtained by tempering a solid pellet at 350 °C. Cs_4SnBr_6 crystallizes in a trigonal crystal system ($R\bar{3}c$

space group; Figure 1b; Supporting Information, Tables S3–S9), wherein $[\text{SnBr}_6]^{4-}$ octahedra are separated by Cs^+ cations. The Cs^+ cations occupy two distinct crystallographic positions (Supporting Information, Figure S3).

Unlike the isostructural Cs_4PbBr_6 , which shows narrow excitonic PL only at low temperatures and at wavelengths < 400 nm,^[16] Cs_4SnBr_6 exhibits broad-band green-yellow PL at RT from STEs (peak maximum at 540 nm, Figure 1c). Upon measuring the PL excitation (PLE) and absorption spectra it was found that Cs_4SnBr_6 resembled a molecular material with a sharp excitation peak at 340 nm yielding a large Stokes shift of about 1.2 eV (Supporting Information, Figure S4). A PLQY of $15 \pm 5\%$ was measured at RT. PLE and PL spectra were found to be tunable through the partial substitution of both A-site cations (Cs with Rb, K) and the halide anions (Br with I). Na was not observed to substitute Cs (Supporting Information, Figure S5).

In $(\text{C}_4\text{N}_2\text{H}_{14}\text{X})_4\text{SnX}_6$ ($\text{X} = \text{Br}/\text{I}$),^[21] the addition of iodide red-shifts both the excitation and STE emission spectra. Similarly, the PL of Cs_4SnX_6 shifts to 620 nm (orange emission) at a Br:I ratio of ca. 1:1 (Figure 2a). In agreement with Vegard's law, a linear change in both the *a* and *c* lattice parameters was observed over the range of compositions from Cs_4SnBr_6 to Cs_4SnI_6 (Supporting Information, Figures S6, S7; Tables S10, S11). Samples with greater than 50% substitution by iodide, however, did not exhibit PL at RT and were not investigated further.

While bromide and iodide occupy the same general position within the structure of Cs_4SnBr_6 , Rb^+ and K^+ could potentially substitute two distinct crystallographic positions of Cs^+ (Supporting Information, Figure S3). Substitution by Rb^+ or K^+ occurred only on the Cs_2 site (1/4 of all Cs, six-fold coordination, Figure 2b; Supporting Information, Figure S8, Tables S12, S13), which explains the observed experimental 25 %-limit for substitution (Supporting Information, Figure S9). Plotting the lattice constants against the molar fractions of K^+ or Rb^+ ions, estimated from Rietveld refinement and energy-dispersive X-ray spectroscopy (EDS), yields a seemingly linear trend for the *c* parameter, in agreement with Vegard's law, whereas the *a* parameter increases only slightly (Figure 2c; Supporting Information, Figures S9–S11). The site affected is part of an infinite chain of $[\text{SnBr}_6]^{4-}$ octahedra separated by $\text{Cs}/\text{Rb}/\text{K}$ ions. Since the chain is oriented parallel to the *c*-axis, substitution by Rb or K will cause the largest effect along this axis resulting in a decrease in the *c* parameter.

The substitution of Cs^+ by Rb^+ or K^+ results in a blue-shift of the PL maximum. This shift is dependent on both the degree of substitution and on the identity of the substituting cation. For 25 % substitution, Rb^+ shifts the PL peak to 519 nm, whereas K^+ yields a PL peak at 500 nm (Figure 2d). Strikingly, the PLE remains unaffected. The same scenario was observed for the other examined Br:I ratios (ca. 5:1, 2:1, 1:1; Figure 2e; Figure S12, Tables S14, S15).

Temperature-dependent PL spectra were measured down to 6 K (Supporting Information, Figures S13, S14). It was found that the PL intensity increased with decreasing temperature and, in the case of Cs_4SnBr_6 , the emission intensity reached a maximum at about 200 K. Given a RT QY of $15 \pm$

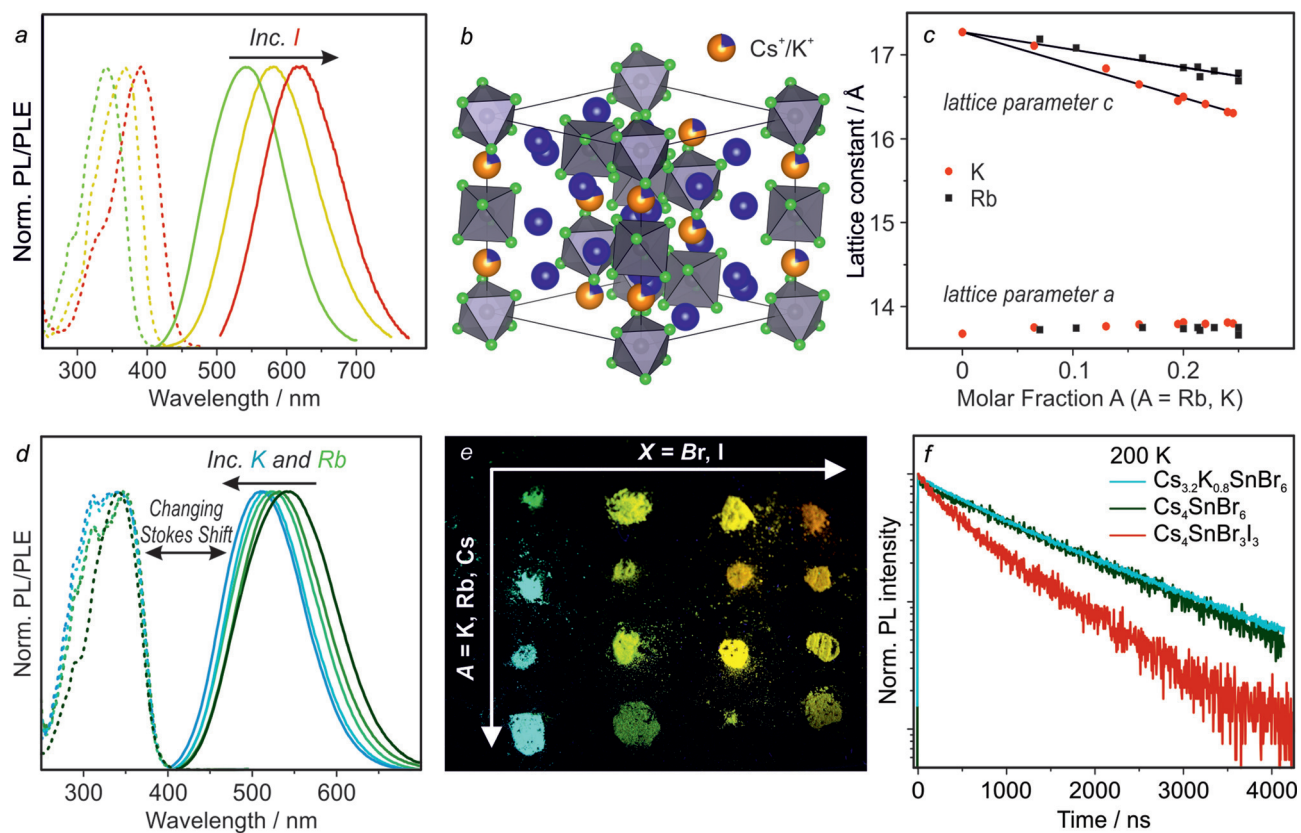


Figure 2. Structural and optical characterization of $\text{Cs}_{4-x}\text{A}_x\text{Sn}(\text{Br},\text{I})_6$ compounds ($\text{A} = \text{K}, \text{Rb}$). a) PL and PLE spectra of $\text{Cs}_4\text{Sn}(\text{Br},\text{I})_6$. b) Crystal structure of $\text{Cs}_{3.2}\text{K}_{0.8}\text{SnBr}_6$ determined by Rietveld refinement. c) The change in the a and c lattice parameters upon Cs^+ substitution by Rb^+ and K^+ . d) PL and PLE spectra for Rb^+ or K^+ substituted compounds. e) Image of $\text{Cs}_{4-x}\text{A}_x\text{Sn}(\text{Br},\text{I})_6$ powders under 365 nm UV light. f) TRPL of Cs_4SnBr_6 , $\text{Cs}_{3.2}\text{K}_{0.8}\text{SnBr}_6$, and $\text{Cs}_4\text{SnBr}_3\text{I}_3$ at 200 K.

5%, the QY of Cs_4SnBr_6 is estimated to be near-unity at 200 K (Supporting Information, Figure S15a). At 6 K, no higher-energy emission, that is, from free excitons, could be observed in Cs_4SnBr_6 or $\text{Cs}_4\text{SnBr}_3\text{I}_3$ (Supporting Information, Figures S14, S15b).

The time-resolved PL (TRPL) of Cs_4SnBr_6 at RT exhibits a monoexponential decay with an average lifetime of 540 ns (Supporting Information, Figure S16). TRPL decays were then recorded at 200 K (the temperature that corresponds to highest QY, Figure 2 f; Supporting Information, Figure S15), and it was observed that the lifetime increased to 1381 ns (1424 ns for K-substitution), while remaining monoexponential (Figure 2 f). Substitution with iodide accelerated the average lifetime (600 ns at 200 K for $\text{Cs}_4\text{SnBr}_3\text{I}_3$, Figure 2 f; see the Supporting Information, Figure S16b for RT comparison). Additionally, the radiative lifetime was found to be insensitive towards dilution with CsBr , excitation intensity, crystallinity, and encapsulation within a UV-curable epoxy (Supporting Information, Figure S16c,d), indicating a lack of surface effects on PL properties in these 0D materials.

Broad-band, strongly Stokes-shifted emission with relatively long radiative lifetimes indicates the formation of STEs (Figure 3 a). As in molecular complexes and similarly small entities, structural changes occur between the ground state and the excited state. Emission from STEs is then somewhat similar to an indirect-gap optical transition since coupling to

phonons is required.^[24] Besides 0D-tin halides,^[21b] emission from STEs has also been observed in 1D- and 2D-layered materials.^[25]

To rationalize the effect of A-site substitution observed in these materials, calculations of the partial density of states (DOS) by density functional theory (DFT) were utilized (Figure 3 b; Supporting Information, Figure S17, Table S16).

A $1 \times 1 \times 1$ unit cell (66 atoms) was used as a model system for Cs_4SnBr_6 , $\text{Cs}_3\text{RbSnBr}_6$, and $\text{Cs}_3\text{KSnBr}_6$ materials. The electronic states were found to be highly localized in all three compositions and the band gap was found to consist of Sn 5s, Br 5p (conduction band/LUMO) and Sn 5p, Br 5p orbitals (valence band/HOMO). A-cation orbitals do not significantly contribute to HOMO and LUMO states (Supporting Information, Figure S17). This is corroborated by the experiment given that A-site substitution did not substantially affect the PLE spectra.

It was previously shown that both tin- and lead-halide octahedra distort significantly upon photoexcitation in low-dimensional materials.^[26] By modeling the excited state and ground state geometries, we find that the extent of distortion was the principle reason for the Stokes shift (Figure 3 b). A pseudo-Jahn-Teller distortion was observed with elongation of up to 17% in the axial Sn–Br bonds, and a contraction of up to 7% in the equatorial bonds. This distortion was found to be greatest in Cs_4SnBr_6 and decreased from Cs^+ to Rb^+ to K^+ .

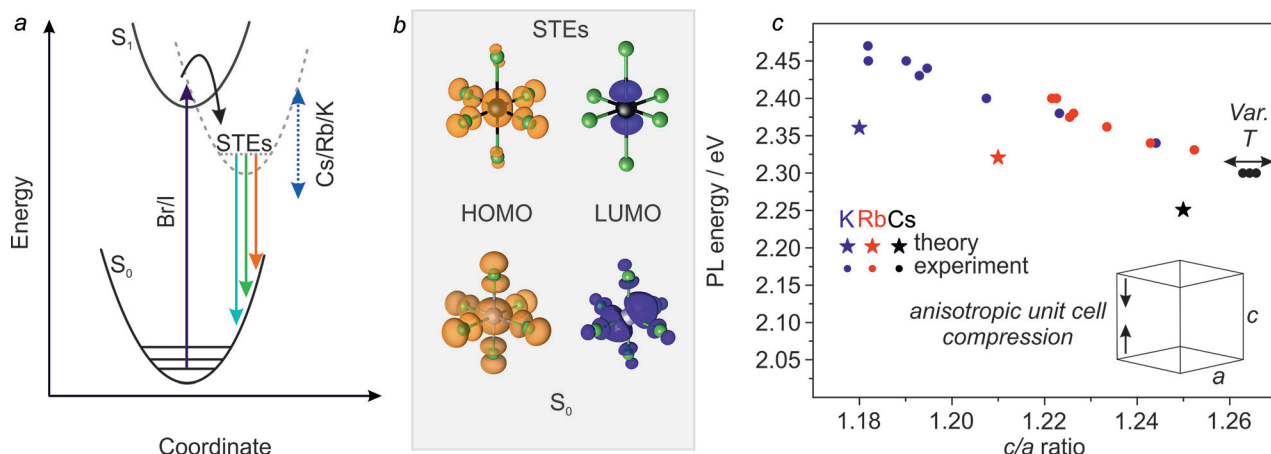


Figure 3. a) Generic configurational coordinate diagram illustrating the origin of STE PL in $\text{Cs}_{4-x}\text{A}_x\text{Sn}(\text{Br}_{1-y}\text{I}_y)_6$. b) Ground-state and excited-state (STE) HOMOs and LUMOs. c) Experimental and theoretical results demonstrating that PL energy varies linearly with the ratio of c-axis to a-axis length. Variable-temperature measurements (three data points; black circles) are plotted for Cs_4SnBr_6 at 100 K, 200 K, and 273 K.

(Supporting Information, Table S17). In other words, the energy required for distortion correlates well with the measured Stokes shift. Larger distortion is allowed by greater distance between the octahedra; primarily along the c -axis. The ratio between the lengths of the c - and a -axes was found to correlate most strongly with PL energy, experimentally and in calculations (Figure 3c). On the other hand, isotropic changes to the unit cell (that is, contraction during cooling) do not affect the PL (Supporting Information, Table S18).

In summary, several new 0D tin halides with the general formula $\text{Cs}_{4-x}\text{A}_x\text{Sn}(\text{Br}_{1-y}\text{I}_y)_6$ have been found to exhibit broad-band RT PL that is tunable from 500 nm to 620 nm. The PL peak position and Stokes shifts can be concomitantly adjusted by the substitution of Cs^+ with either Rb^+ or K^+ as well as Br^- by I^- . PL properties were rationalized by the DFT analysis of STEs. Future studies might concern applications of such materials in luminescent solar concentrators and light emitting devices, harnessing their structural tunability and fully inorganic compositions.

Experimental Section

Materials and methods are included in the Supporting Information. Further details on the crystal structure investigation may be obtained from the Fachinformationszentrum Karlsruhe, 76344 Eggenstein-Leopoldshafen, Germany (fax: (+49) 7247-808-666; e-mail: crysdata@fiz-karlsruhe.de), on quoting the depository numbers CSD-434641, 434642, 434643, 434644, 434645, 434646, and 434647.

Acknowledgements

We thank Dr. F. Krumeich for EDS measurements and acknowledge the support of the Scientific Center for Optical and Electron Microscopy (ScopeM) of the Swiss Federal Institute of Technology ETHZ. We thank Michael Solar for single-crystal X-ray diffraction measurements. This work was financially supported by the European Union through the FP7 (ERC Starting Grant NANOSOLID, GA No. 306733)

and through the Horizon-2020 (Marie-Skłodowska Curie ITN network PHONSI, H2020-MSCA-ITN-642656). Authors thank IBM-Zurich Research, in particular Dr. T. Stöferle and Dr. R. F. Mahrt, for support with low-temperature PL experiments. I.I. would like to thank The Netherlands Organization of Scientific Research (NWO) for providing financial support within the Innovative Research Incentive (Vidi) Scheme (Grant no. 723.013.002). DFT calculations were carried out on the Dutch national e-infrastructure with the support of SURF Cooperative.

Conflict of interest

The authors declare no conflict of interest.

Keywords: luminescence · perovskites · self-trapped excitons · solid-state synthesis · tin

How to cite: *Angew. Chem. Int. Ed.* **2018**, *57*, 11329–11333
Angew. Chem. **2018**, *130*, 11499–11503

- [1] a) D. B. Mitzi, C. A. Felid, W. T. A. Harrison, A. M. Guloy, *Nature* **1994**, *369*, 467–469; b) D. B. Mitzi, K. Liang, S. Wang, *Inorg. Chem.* **1998**, *37*, 321–327; c) Z. Xu, D. B. Mitzi, *Inorg. Chem.* **2003**, *42*, 6589–6591; d) L. Pedesseau, D. Sapori, B. Traore, R. Robles, H. H. Fang, M. A. Loi, H. Tsai, W. Nie, J. C. Blancon, A. Neukirch, S. Tretiak, A. D. Mohite, C. Katan, J. Even, M. Kepenekian, *ACS Nano* **2016**, *10*, 9776–9786; e) L. Mao, H. Tsai, W. Nie, L. Ma, J. Im, C. C. Stoumpos, C. D. Malliakas, F. Hao, M. R. Wasielewski, A. D. Mohite, M. G. Kanatzidis, *Chem. Mater.* **2016**, *28*, 7781–7792; f) C. C. Stoumpos, D. H. Cao, D. J. Clark, J. Young, J. M. Rondinelli, J. I. Jang, J. T. Hupp, M. G. Kanatzidis, *Chem. Mater.* **2016**, *28*, 2852–2867; g) H. Tsai, W. Nie, J. C. Blancon, C. C. Stoumpos, R. Asadpour, B. Harutyunyan, A. J. Neukirch, R. Verduzco, J. J. Crochet, S. Tretiak, L. Pedesseau, J. Even, M. A. Alam, G. Gupta, J. Lou, P. M. Ajayan, M. J. Bedzyk, M. G. Kanatzidis, *Nature* **2016**, *536*, 312–316; h) L. Mao, Y. Wu, C. C. Stoumpos, M. R. Wasielewski, M. G. Kanatzidis, *J. Am. Chem. Soc.* **2017**, *139*, 5210–5215; i) L. Mao, Y. Wu, C. C. Stoumpos, B. Traore, C. Katan, J. Even, M. R. Wasielewski, M. G. Kanatzidis, *J. Am. Chem. Soc.* **2017**, *139*,

- 11956–11963; j) D. H. Cao, C. C. Stoumpos, T. Yokoyama, J. L. Logsdon, T.-B. Song, O. K. Farha, M. R. Wasielewski, J. T. Hupp, M. G. Kanatzidis, *ACS Energy Lett.* **2017**, *2*, 982–990; k) C. M. M. Soe, C. C. Stoumpos, M. Kepenekian, B. Traore, H. Tsai, W. Nie, B. Wang, C. Katan, R. Seshadri, A. D. Mohite, J. Even, T. J. Marks, M. G. Kanatzidis, *J. Am. Chem. Soc.* **2017**, *139*, 16297–16309; l) O. Nazarenko, M. R. Kotyrb, M. Worle, E. Cuervo-Reyes, S. Yakunin, M. V. Kovalenko, *Inorg. Chem.* **2017**, *56*, 11552–11564; m) C. C. Stoumpos, L. Mao, C. D. Malliakas, M. G. Kanatzidis, *Inorg. Chem.* **2017**, *56*, 56–73; n) O. Nazarenko, M. R. Kotyrb, S. Yakunin, M. Aebl, G. Raino, B. M. Benin, M. Worle, M. V. Kovalenko, *J. Am. Chem. Soc.* **2018**, *140*, 3850–3853; o) M. D. Smith, H. I. Karunadasa, *Acc. Chem. Res.* **2018**, *51*, 619–627.
- [2] a) M. I. Saidaminov, O. F. Mohammed, O. M. Bakr, *ACS Energy Lett.* **2017**, *2*, 889–896; b) H. Lin, C. Zhou, Y. Tian, T. Siegrist, B. Ma, *ACS Energy Lett.* **2018**, *3*, 54–62; c) Q. A. Akkerman, A. L. Abdelhady, L. Manna, *J. Phys. Chem. Lett.* **2018**, *9*, 2326–2337.
- [3] a) M. A. Green, A. Ho-Baillie, H. J. Snaith, *Nat. Photonics* **2014**, *8*, 506–514; b) J. S. Manser, J. A. Christians, P. V. Kamat, *Chem. Rev.* **2016**, *116*, 12956–13008; c) Q. A. Akkerman, G. Raino, M. V. Kovalenko, L. Manna, *Nat. Mater.* **2018**, *17*, 394–405.
- [4] S. Yakunin, Y. Shynkarenko, D. N. Dirin, I. Cherniukh, M. V. Kovalenko, *NPG Asia Mater.* **2017**, *9*, e431.
- [5] a) X. Hu, X. Zhang, L. Liang, J. Bao, S. Li, W. Yang, Y. Xie, *Adv. Funct. Mater.* **2014**, *24*, 7373–7380; b) L. Dou, Y. M. Yang, J. You, Z. Hong, W. H. Chang, G. Li, Y. Yang, *Nat. Commun.* **2014**, *5*, 1–6.
- [6] S. Yakunin, M. Sytnyk, D. Kriegner, S. Shrestha, M. Richter, G. J. Matt, H. Azimi, C. J. Brabec, J. Stangl, M. V. Kovalenko, W. Heiss, *Nat. Photonics* **2015**, *9*, 444–449.
- [7] a) C. C. Stoumpos, C. D. Malliakas, J. A. Peters, Z. Liu, M. Sebastian, J. Im, T. C. Chasapis, A. C. Wibowo, D. Y. Chung, A. J. Freeman, B. W. Wessels, M. G. Kanatzidis, *Cryst. Growth Des.* **2013**, *13*, 2722–2727; b) S. Yakunin, D. N. Dirin, Y. Shynkarenko, V. Morad, I. Cherniukh, O. Nazarenko, D. Kreil, T. Nauser, M. V. Kovalenko, *Nat. Photonics* **2016**, *10*, 585–589.
- [8] a) M. M. Lee, J. Teuscher, T. Miyasaka, T. N. Murakami, H. J. Snaith, *Science* **2012**, *338*, 643–647; b) J. Burschka, N. Pellet, S. J. Moon, R. Humphry-Baker, P. Gao, M. K. Nazeeruddin, M. Gratzel, *Nature* **2013**, *499*, 316–319.
- [9] Z.-K. Tan, R. S. Moghaddam, M. L. Lai, P. Docampo, R. Higler, F. Deschler, M. Price, A. Sadhanala, L. M. Pazos, D. Credgington, F. Hanusch, T. Bein, H. J. Snaith, R. H. Friend, *Nat. Nanotechnol.* **2014**, *9*, 687–692.
- [10] a) R. E. Brandt, V. Stevanović, D. S. Ginley, T. Buonassisi, *MRS Commun.* **2015**, *5*, 265–275; b) O. Yaffe, Y. Guo, L. Z. Tan, D. A. Egger, T. Hull, C. C. Stoumpos, F. Zheng, T. F. Heinz, L. Kronik, M. G. Kanatzidis, J. S. Owen, A. M. Rappe, M. A. Pimenta, L. E. Brus, *Phys. Rev. Lett.* **2017**, *118*, 136001; c) K. Miyata, T. L. Atallah, X.-Y. Zhu, *Sci. Adv.* **2017**, *3*, e1701469.
- [11] a) L. C. Schmidt, A. Pertegas, S. Gonzalez-Carrero, O. Malinkiewicz, S. Agouram, G. Minguez Espallargas, H. J. Bolink, R. E. Galian, J. Perez-Prieto, *J. Am. Chem. Soc.* **2014**, *136*, 850–853; b) L. Protesescu, S. Yakunin, M. I. Bodnarchuk, F. Krieg, R. Caputo, C. H. Hendon, R. X. Yang, A. Walsh, M. V. Kovalenko, *Nano Lett.* **2015**, *15*, 3692–3696; c) D. N. Dirin, L. Protesescu, D. Trummer, I. V. Kochetygov, S. Yakunin, F. Krumeich, N. P. Stadie, M. V. Kovalenko, *Nano Lett.* **2016**, *16*, 5866–5874; d) Q. A. Akkerman, S. G. Motti, A. R. Srimath Kandada, E. Mosconi, V. D'Innocenzo, G. Bertoni, S. Marras, B. A. Kamino, L. Miranda, F. De Angelis, A. Petrozza, M. Prato, L. Manna, *J. Am. Chem. Soc.* **2016**, *138*, 1010–1016; e) H. Huang, Q. Xue, B. Chen, Y. Xiong, J. Schneider, C. Zhi, H. Zhong, A. L. Rogach, *Angew. Chem. Int. Ed.* **2017**, *56*, 9571–9576; *Angew. Chem.* **2017**, *129*, 9699–9704; f) L. Protesescu, S. Yakunin, O. Nazarenko, D. N. Dirin, M. V. Kovalenko, *ACS Appl. Nano Mater.* **2018**, *1*, 1300–1308.
- [12] M. Chen, M.-G. Ju, A. D. Carl, Y. Zong, R. L. Grimm, J. Gu, X. C. Zeng, Y. Zhou, N. P. Padture, *Joule* **2018**, *2*, 558–570.
- [13] a) B. Kang, K. Biswas, *J. Phys. Chem. C* **2016**, *120*, 12187–12195; b) R. Král, V. Babin, E. Mihóková, M. Buryi, V. V. Laguta, K. Nitsch, M. Nikl, *J. Phys. Chem. C* **2017**, *121*, 12375–12382.
- [14] K. Saeki, Y. Fujimoto, M. Koshimizu, D. Nakauchi, H. Tanaka, T. Yanagida, K. Asai, *Jpn. J. Appl. Phys.* **2018**, *57*, 030310.
- [15] N. Sakai, A. A. Haghimirad, M. R. Filip, P. K. Nayak, S. Nayak, A. Ramadan, Z. Wang, F. Giustino, H. J. Snaith, *J. Am. Chem. Soc.* **2017**, *139*, 6030–6033.
- [16] M. Nikl, E. Mihóková, K. Nitsch, F. Somma, C. Giampaolo, G. P. Pazzi, P. Fabeni, S. Zazubovich, *Chem. Phys. Lett.* **1999**, *306*, 280–284.
- [17] a) B. Lee, C. C. Stoumpos, N. Zhou, F. Hao, C. Malliakas, C. Y. Yeh, T. J. Marks, M. G. Kanatzidis, R. P. Chang, *J. Am. Chem. Soc.* **2014**, *136*, 15379–15385; b) A. Kaltzoglou, M. Antoniadou, A. G. Kontos, C. C. Stoumpos, D. Perganti, E. Siranidi, V. Raptis, K. Trohidou, V. Psycharis, M. G. Kanatzidis, P. Falaras, *J. Phys. Chem. C* **2016**, *120*, 11777–11785.
- [18] a) R. Wernicke, H. Kupka, W. Ensslin, H.-H. Schmidtkne, *Chem. Phys.* **1980**, *47*, 235–244; b) G. Blasse, G. J. Dirksen, W. Abriel, *Chem. Phys. Lett.* **1987**, *136*, 460–464; c) T. V. Sedakova, A. G. Mirochnik, V. E. Karasev, *Opt. Spectrosc.* **2011**, *110*, 755–761; d) B. V. Bukvetskii, T. V. Sedakova, A. G. Mirochnik, *Russ. J. Coord. Chem.* **2012**, *38*, 106–110.
- [19] a) T. V. Sedakova, A. G. Mirochnik, V. E. Karasev, *Opt. Spectrosc.* **2008**, *105*, 517–523; b) V. I. Vovna, A. A. Dotsenko, V. V. Korochentsev, O. L. Shcheka, I. S. Os'mushko, A. G. Mirochnik, T. V. Sedakova, V. I. Sergienko, *J. Mol. Struct.* **2015**, *1091*, 138–146; c) C. Zhou, M. Worku, J. Neu, H. Lin, Y. Tian, S. Lee, Y. Zhou, D. Han, S. Chen, A. Hao, P. I. Djurovich, T. Siegrist, M.-H. Du, B. Ma, *Chem. Mater.* **2018**, *30*, 2374–2378.
- [20] N. Elfaleh, S. Kamoun, *J. Organomet. Chem.* **2016**, *819*, 95–102.
- [21] a) C. Zhou, Y. Tian, Z. Yuan, H. Lin, B. Chen, R. Clark, T. Dilbeck, Y. Zhou, J. Hurley, J. Neu, T. Besara, T. Siegrist, P. Djurovich, B. Ma, *ACS Appl. Mater. Interfaces* **2017**, *9*, 44579–44583; b) C. Zhou, H. Lin, Y. Tian, Z. Yuan, R. Clark, B. Chen, L. J. van de Burgt, J. C. Wang, Y. Zhou, K. Hanson, Q. J. Meisner, J. Neu, T. Besara, T. Siegrist, E. Lambers, P. Djurovich, B. Ma, *Chem. Sci.* **2018**, *9*, 586–593.
- [22] a) R. H. Andrews, S. J. Clark, J. D. Donaldson, *J. Chem. Soc. Dalton Trans.* **1983**, 767–770; b) S. V. Myagkota, P. V. Savchin, A. S. Voloshinovskii, T. M. Demkiv, Y. V. Boiko, R. S. Vus, L. S. Demkiv, *Phys. Solid State* **2008**, *50*, 1473–1476.
- [23] M. Hu, C. Ge, J. Yu, J. Feng, *J. Phys. Chem. C* **2017**, *121*, 27053–27058.
- [24] K. Thirumal, W. K. Chong, W. Xie, R. Ganguly, S. K. Muduli, M. Sherburne, M. Asta, S. Mhaisalkar, T. C. Sum, H. S. Soo, N. Mathews, *Chem. Mater.* **2017**, *29*, 3947–3953.
- [25] a) E. R. Dohner, A. Jaffe, L. R. Bradshaw, H. I. Karunadasa, *J. Am. Chem. Soc.* **2014**, *136*, 13154–13157; b) Z. Yuan, C. Zhou, Y. Tian, Y. Shu, J. Messier, J. C. Wang, L. J. van de Burgt, K. Kountouriotis, Y. Xin, E. Holt, K. Schanze, R. Clark, T. Siegrist, B. Ma, *Nat. Commun.* **2017**, *8*, 1–7; c) M. D. Smith, B. L. Watson, R. H. Dauskardt, H. I. Karunadasa, *Chem. Mater.* **2017**, *29*, 7083–7087.
- [26] a) C. Zhou, H. Lin, H. Shi, Y. Tian, C. Pak, M. Shatruk, Y. Zhou, P. Djurovich, M. H. Du, B. Ma, *Angew. Chem. Int. Ed.* **2018**, *57*, 1021–1024; *Angew. Chem.* **2018**, *130*, 1033–1036; b) B. Kang, K. Biswas, *J. Phys. Chem. Lett.* **2018**, *9*, 830–836.

Manuscript received: June 5, 2018

Revised manuscript received: July 6, 2018

Accepted manuscript online: July 12, 2018

Version of record online: July 30, 2018